

Suppression of spin-polarization in graphene nanoribbon by edge defect and impurity

Bing Huang¹, Feng Liu^{2*}, Jian Wu¹, Bing-Lin Gu¹, and Wenhui Duan^{1†}

¹*Department of Physics, Tsinghua University, Beijing 100084, PRC and*

²*Department of Materials Science and Engineering,
University of Utah, Salt Lake City, Utah 84112*

(Dated: April 7, 2019)

Abstract

We investigate the effect of edge defects (vacancies) and impurities (substitutional dopants) on the robustness of spin-polarization in graphene nanoribbons (GNRs) with zigzag edges, using density-functional-theory calculations. We found that the stability of the spin state and its magnetic moments decrease continuously with increasing concentration of defects or impurities. The system generally becomes non-magnetic at the concentration of one edge defect (impurity) per ~ 10 Å. The spin suppression is shown to be caused by reduction and removal of edge states at the Fermi energy. Our analysis implies an important criterion on the GNR samples for spintronics applications.

PACS numbers: 75.75.+a,73.22.-f,75.30.Hx

* Email: fliu@eng.utah.edu

† Email: dwh@phys.tsinghua.edu.cn

Graphene nanoribbons (GNRs) have attracted much recent interest because of their unique electronic properties and vast potential for device applications [1, 2, 3, 4, 5, 6, 7, 8, 9, 10, 11]. On one hand, they resemble the carbon nanotubes (CNTs), having the electronic properties tunable by the ribbon width and direction due to quantum confinement. On the other hand, they differ from the CNTs, having the free edges that give rise to new electronic signatures of edge states [1]. The existence of free edges makes the GNRs more accessible to doping [7] and chemical modification [10], but also more susceptible to structural defects and impurities [9, 11].

Of particular interest are those GNRs with zigzag edges, which are shown to have a spin-polarized ground state by various theoretical calculations [4, 5, 8]. The spin-polarization is originated from the edge states that introduce a high density of state at Fermi energy. It can be qualitatively understood in terms of Stoner magnetism of sp electrons (in analogy to conventional d electrons) occupying a very narrow edge band to render an instability of spin-band splitting [12]. The spins are found to be localized on the ribbon edges, with ferromagnetic coupling within each edge and antiferromagnetic coupling between the two edges.

Because the magnetism in GNRs is resulted from the highly degenerate edge states, it must require a perfect edge structure. However, real samples of GNRs [9] are unlikely to have perfect edges but contain structural defects and impurities of foreign atomic species. Naturally, one important question is how robust is the spin state in presence of edge defects and impurities. The answer to this question not only is scientifically interesting to better understand the physical mechanisms of spin-polarization in GNRs, but also have important technological implications if GNRs are to be realized as a new class of spintronic materials. Here, using first-principles density-functional-theory (DFT) calculations, we present a systematic study of the stability and degree of spin-polarization in GNRs as a function of the concentration of edge defects and impurities.

We have chosen the vacancy and the substitutional boron (B) atom, as typical examples of structural edge defect and impurity, respectively, based on the consideration that vacancies are expected to be the most abundant defects in a roughened edge and B atoms are a common choice of electronic dopants [6, 7]. Our calculations show that in the presence of either vacancy or B impurity, the spin-polarization is completely suppressed at the defect (impurity) sites, while it may preserve on those sites away from defects (impurities) when

the defect (impurity) concentration is low. The stability of the spin state and its "average" magnetic moment decreases continuously with increasing defect (impurity) concentration. If the defects (impurities) are uniformly distributed on the edge, typically the system becomes non-magnetic at the concentration of one edge defect (impurity) per $\sim 10 \text{ \AA}$, i.e., when the defects (impurities) are at the fourth nearest-neighbor (NN) positions or closer. The magnetism may also be "dead" locally in between two defects (impurities) when they are closer than the third NN positions. The spin suppression correlates closely with the reduction and removal of edge states at the Fermi energy.

Our calculations are performed using DFT pseudopotential plane-wave method within the local spin density approximation[13]. The plane wave cut-off energy is set as 450 eV. The structure optimization has been performed until the residual atomic forces are less than 0.01 eV/ \AA . We calculated GNRs with H-terminated zigzag edges of two different widths, namely the (3,3) and (2,2) "armchair" ribbons [7], using a nomenclature in analogy to armchair carbon nanotubes that would unfold into corresponding ribbons with zigzag edges. Vacancies or impurities are introduced in the edge by removing edge C-H pairs or replacing C with B, respectively. Their concentrations are varied from 0.034 \AA^{-1} to 0.136 \AA^{-1} along the edge, and both uniform and non-uniform distributions of defects (impurities) are considered.

Figure 1a shows the calculated ground-state spin distributions of a (3,3) GNR at an edge vacancy concentration of 0.034 \AA^{-1} . The spin polarization is mostly localized on the edges with the top and bottom edge spins anti-ferromagnetic coupled with each other. One notices that spin is locally absent at the vacancy sites and it increases as one moves away from the vacancy along the edge. Figure 1b shows the ground-state spin distributions at a higher vacancy concentration of 0.068 \AA^{-1} . Overall, the spins exhibit an identical distribution pattern, but their magnitude is reduced in comparison to Fig. 1a. At even higher vacancy concentration of 0.136 \AA^{-1} , Figure 1c shows that the spins are completely suppressed at all atomic sites and the GNR becomes non-magnetic. Almost identical results are obtained for B impurities as shown in Figs. 1d-1f.

In Fig. 1g, we plot the magnetic moments on the top edge as a function of edge positions, at four different vacancy concentrations. Without vacancy, there is a uniform spin distribution with a large moment of $0.22\mu_B$ at every edge sites (red squares). When vacancies are introduced at a low enough concentration so that spins preserve on the edges, the presence of vacancies in effect enforces a spin-density wave (oscillation) along the ribbon edge, with

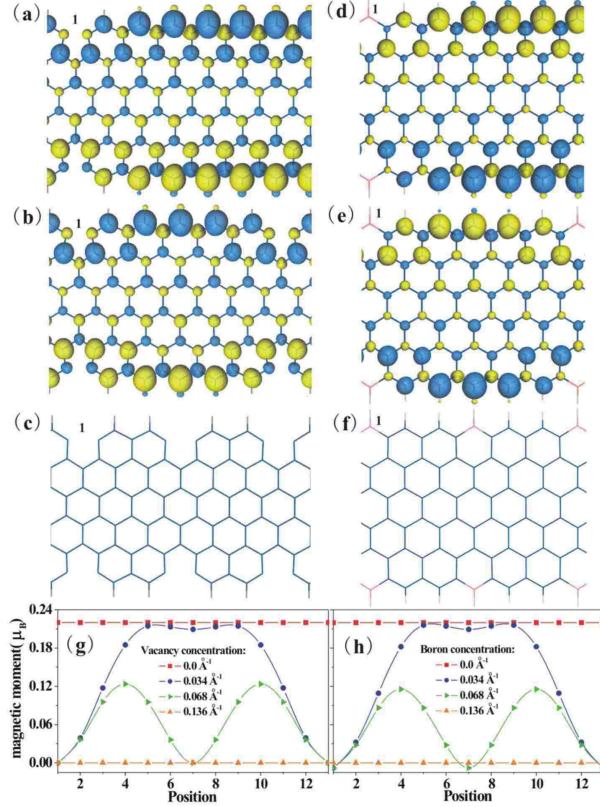


FIG. 1: Isovalue surfaces of charge difference between the spin-up and spin-down states of the ground states calculated for the (3,3) GNR at there different linear vacancy concentrations on the edge: (a) 0.034 \AA^{-1} , (b) 0.068 \AA^{-1} , and (c) 0.136 \AA^{-1} . Half of the supercell in Fig. 1a, one in Fi.g 1b and two in Fig. 1c are shown. The yellow and blue surface represents spin-up and spin-down state, respectively. The range of isovalues is set at $[-0.005:0.005] \mu_B \text{ \AA}^{-1}$ in case (a) and $[-0.003:0.003] \mu_B \text{ \AA}^{-1}$ in case of (b) and (c). (d)-(f) The same as (a)-(c) for B impurities. (g) The magnetic moment per edge atom on the top edge, at there vacancy concentrations corresponding to the case of (a), (b) and (c), plus the case without vacancy. (h)The same as (g) for B impurities.

the zero moment (nodal point) at the vacancy site and the maximum moment at the middle point between the vacancies (blue dots and green right triangles). The period of the spin density wave equals the inverse of vacancy concentration, while its amplitude decreases with increasing concentration. At a sufficiently high concentration, the vacancies suppress all the spins and the moments become zero everywhere (orange up triangle). The same results are obtained for B impurities, as shown in Fig. 1h.

The results in Fig. 1 indicate that the spin-polarization decreases with increasing edge

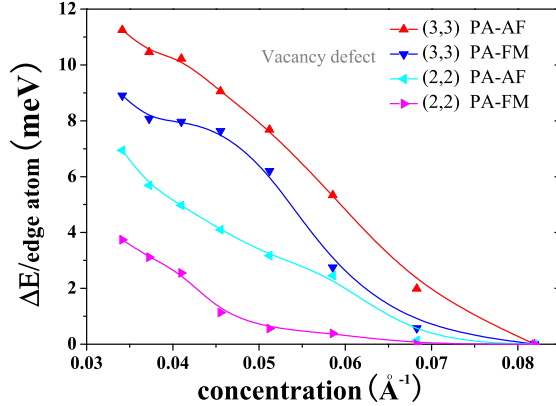


FIG. 2: The energy difference per edge atom between the magnetic (AF or FM) and paramagnetic (PA) state as a function of vacancy concentration in the edge. Two different ribbon widths are shown.

defect (impurity) concentration and eventually vanishes. To further demonstrate this phenomenon, we have compared the relative stability of the spin state with the non-spin state by calculating their energy difference. Figure 2 shows the calculated energy difference per edge atom as a function of vacancy concentration. The results of B impurities are essentially the same. In general, the anti-ferromagnetic (AF) state (with opposite spins at the two edges) is more stable than the ferromagnetic (FM) state (with the same spins at the two edges), and both these magnetic states are more stable than the paramagnetic state (PA). However, the energy difference between the magnetic state and the nonmagnetic state decreases rapidly with increasing defect (impurity) concentration. Eventually, the difference decreases to zero and the GNR becomes nonmagnetic. The critical defect (impurity) concentration for the magnetic to nonmagnetic transition depends on ribbon width. It is lower for a narrower ribbon, e.g., at 0.068 \AA^{-1} for a (2,2) ribbon, and higher for a wider ribbons, e.g., at 0.081 \AA^{-1} for a (3,3) ribbon. For even wider GNRs with a width as large as 3.0 nm, we found that the spin-polarization can still be completely suppressed by defects or impurities at a concentration of $\sim 0.10 \text{ \AA}^{-1}$. It corresponds to an average defect-defect (or impurity-impurity) separation at the fourth NN positions on the edge.

The magnetism is resulted from a high density of state (DOS) at the Fermi Energy (E_F) that renders an instability of spin polarization. Consequently, one expects the suppression

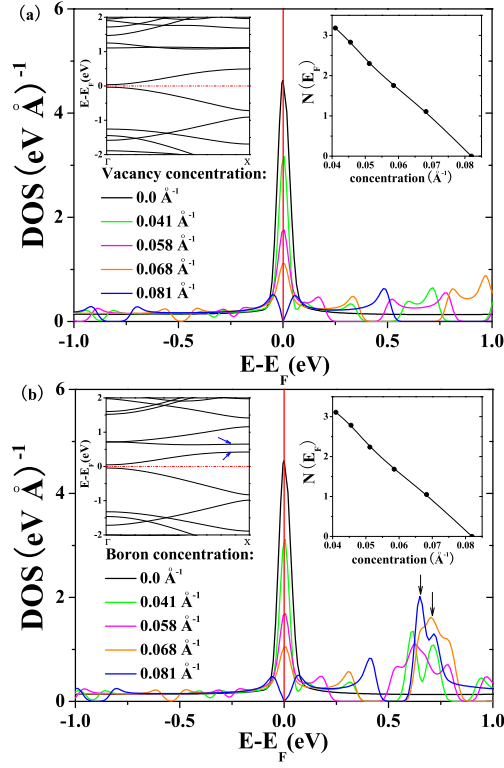


FIG. 3: (a) The calculated total DOS for a (3,3) ribbon in the paramagnetic state at five different vacancy edge concentration. Up-left inset: the band structure at the vacancy concentration of 0.081 \AA^{-1} . Up-right inset: the DOS at E_F ($E=0$) as a function of vacancy concentration. (b) The same as (a) for B impurities.

of magnetism is correlated with the change of DOS at E_F induced by defects (impurities). We have examined the DOS as a function of defect (impurity) concentration, which has indeed confirmed such mechanism. In Fig. 3a, we plot the DOS in the paramagnetic state of the (3,3) ribbon as a function of vacancy concentration. Clearly, the DOS at E_F decreases almost linearly (up-right inset) with increasing vacancy concentration, in close correlation with the magnetization shown in Fig. 1 and 2. As the defect concentration reaches 0.081 \AA^{-1} , the DOS at E_F falls to zero, and the system becomes non-magnetic. Without defects, the highly degenerate edge states in a perfect ribbon edge give rise to the high DOS at E_F . Since the vacancies will not contribute to the same edge state, their presence decreases the DOS at E_F .

Similarly, in Fig. 3b, we plot the DOS in the paramagnetic state of the (3,3) ribbon as a function of B impurity concentration. Again, the DOS at E_F decreases almost linearly (up-right inset) with increasing B concentration and eventually vanishes, so that the ribbon becomes nonmagnetic. However, here the mechanism of DOS reduction at E_F is slightly different from the case of vacancy. The impurity B atoms act as electronic dopants to introduce impurity states (levels) away from the Fermi energy so as to reduce the DOS at E_F . This can be seen in Fig. 3b when the DOS at E_F decreases and vanishes at $E = 0$ with increasing B concentration, another peak of DOS appears and increases at $E = 0.7\text{eV}$. Those bands of edge states (up-left inset) being shifted to 0.7 eV are indicated by arrows. So effectively, the B impurities lift the degeneracy of edge states and hence decrease the DOS at E_F . In addition, the corresponding band structure (up-left inset) shows the system becomes semiconducting with a small band gap upon B doping. (We have also studied the case of N atoms, which showed the same effect as B atoms, except the impurity edge states were shifted to below Fermi energy since N is a *n*-type dopant.)

We may further understand the spin suppression by edge defect (impurity) in the context of itinerant ferromagnetism and local order [14, 15, 16]. It has been shown that the magnetic moment in an itinerant magnetic materials depends strongly on local coordination[14, 15]. When a nonmagnetic "impurity" is introduced in the magnetic medium, the moment is greatly suppressed at the impurity site and its vicinity[15]. Conversely, when a magnetic element is introduced in a nonmagnetic medium, its moment is quenched at low concentration but can be redeveloped at high concentration and there is strong correlation between the magnetic dopants[16].

Similarly, our case here can be thought of doping the magnetic medium of itinerant *sp* electrons [12] with nonmagnetic impurities, vacancy or B atom, which will suppress the magnetic moment at the impurity site and its vicinity. When two and more impurities are introduced, the correlation between them would determine the local state of moment (spin-polarization). To test this idea, we have examined the local magnetic moment in between two defects (or impurities) as a function of their separation. From Fig. 4a to 4c, we see that the local moment in between the two vacancies decreases as the two vacancies moving closer and completely vanishes when they are at the third NN position (Fig. 4c). The same result is also obtained at even lower defect concentrations. This means spin suppression is a rather localized effect. For example, we can selectively introduce defects (impurities) in

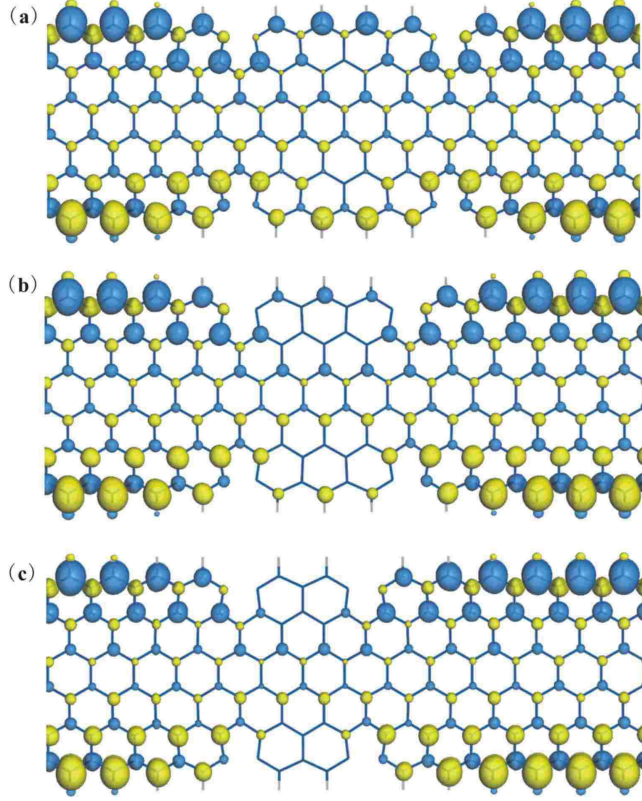


FIG. 4: Similar to Fig. 1a, but with the vacancies moving closer from (a) the fifth NN position (even distribution) to (b) the fourth NN position and to (c) the third NN position. The range of isovalues is set at $[-0.004:0.004] \mu_B \text{ \AA}^{-1}$.

only one ribbon edge while keep the other edge perfect. Then we will create a ferromagnetic order along one ribbon edge while the other edge is nonmagnetic, as shown in Fig. 5, which could be useful for spintronics applications if only ferromagnetism is desirable.

In conclusion, we have examined the robustness of spin-polarization in GNRs with zigzag edge, using first principle calculations. We show that the spin polarization can be greatly suppressed in the presence of edge defects and impurities. In general, the GNR becomes nonmagnetic at a typical edge defect (impurity) concentration of $\sim 0.10 \text{ \AA}^{-1}$ assuming a uniform distribution. The magnetic moments may also vanish locally if two defects (impurities) are closer than the third NN distance. The spin suppression correlates closely with the reduction of DOS at the Fermi energy induced by defects (impurities). It can be qualitatively understood in the context of itinerant magnetism and local order. Our findings also have important technology implications: on one hand providing a potential method for ma-

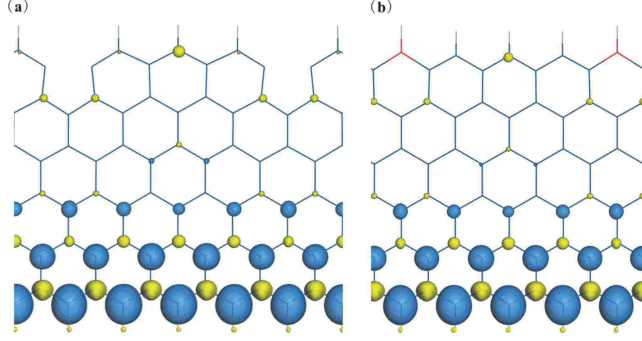


FIG. 5: Similar to Fig. 1a, but with (a) vacancy and (b) B impurity introduced at only one of the two ribbon edges at the fourth NN positions. The range of isovalues is set at $[-0.005:0.005] \mu_B \text{ \AA}^{-1}$.

nipulating the spin state in GNRs, and on the other hand setting up a stringent requirement on the GNR samples for spintronics applications.

The work at Tsinghua is supported by the Ministry of Science and Technology of China and NSFC, the work at Utah is supported by DOE.

-
- [1] K. Nakada, M. Fujita, G. Dresselhaus, and M. S. Dresselhaus, *Phys. Rev. B.* **54**, 17954 (1996).
 - [2] K. Wakabayashi, M. Fujita, H. Ajiki, and M. Sigrist, *Phys. Rev. B.* **59**, 8271 (1999).
 - [3] K. Kusakabe and M. Maruyama, *Phys. Rev. B.* **67**, 092406 (2003).
 - [4] H. Lee, Y. -W. Son, N. Park, S. Han and J. Yu, *Phys. Rev. B.* **72**, 174431 (2005).
 - [5] Y. -W. Son, M. L. Cohen, and S. G. Louie, *Nature (London)* **444**, 347 (2006); *Phys. Rev. Lett.* **97**, 216803 (2006).
 - [6] T. B. Martins, R. H. Miwa, Antonio J. R. da Silva, and A. Fazzio, *Phys. Rev. Lett.* **98**, 196803(2007).
 - [7] Q. M. Yan, B. Huang, J. Yu, F. W. Zheng, J. Zang, J. Wu, B. L. Gu, F. Liu and W. H. Duan, *Nano Lett.* **7**, 1469 (2007)
 - [8] L. Pisani, J. A. Chan, B. Montanari, and N. M. Harrison, *Phys. Rev. B.* **75**, 064418 (2007).
 - [9] M. Y. Han, B. Oezylmaz, Y. Zhang, and P. Kim, *Phys. Rev. Lett.* **98**, 206805 (2007).
 - [10] O. Hod, V. Barone, J. E. Peralta, and G. E. Scuseria, *Nano Lett.* in press (2007).
 - [11] D. Gunlycke, D. A. Areshkin, and C. T. White, *Appl. Phys. Lett.* **90**, 142104 (2007).

- [12] D. M. Edwards and M. I. Katsnelson. *J. Phys.: Condens. Matter* **18**, 7209 (2006).
- [13] G. Kresse and J. Furthmüller, *Comput. Mater. Sci.* **6**, 15 (1996).
- [14] F. Liu, M. R. Press, S. N. Khanna, and P. Jena, *Phys. Rev. B.* **39**, 6914 (1989).
- [15] M. R. Press, F. Liu, S. N. Khanna, and P. Jena, *Phys. Rev. B.* **40**, 399 (1989).
- [16] F. Liu, S. N. Khanna, L. Magaud, P. Jena, V. de Coulon, F. Reuse, S. S. Jaswal, X.-G. He, and F. Cyrot-Lackman, *Phys. Rev. B.* **48**, 1295 (1993).